Fenske-Hall calculation on $B_{32}H_{32}^{2-}$ shows that the HOMO has T_{1g} symmetry and belongs to the odd $\bar{H}^{\pi}$ set of π orbitals. Its conjugate T_{1u} partner, belonging to the H^{π} set, is the LUMO of this cluster, and lies about 1 eV above the HOMO. Hence we see that for this highly symmetrical species, with only two types of vertex atom, the odd and even π sets do indeed overlap.

Conclusions

In this paper we have discussed the splitting of cluster orbitals using the framework of Stone's tensor surface harmonic (TSH) theory. Although the TSH theory cluster orbitals do not transform like their parent spherical harmonics under *arbitrary* rotations, we still expect the splitting patterns to be qualitatively similar. In particular, when the electron-nucleus potential energy is expanded in spherical harmonics a center-of-gravity rule may be deduced for the first-order splitting of the spherical harmonics, $Y_{L,M}$, by the non spherically symmetric part of the Hamiltonian.

The splittings of cluster orbitals are found to depend upon the relation between the nodal surfaces of the nonzero terms in the spherical harmonic expansion and the cluster vertices. Hence we have discussed the relation between the *shape* of a cluster and its energy level spectrum with particular reference to the *closo*-borohydrides. The shape of the molecule determines the *sense* of the cluster orbital splittings as well as the *magnitude* of the nonzero terms in the potential energy expansion. These expectations are illustrated by the different electron counts of toroidal and spherical gold clusters and are also expected to influence the skeletal rearrangements of these species.

Some of the techniques used have direct analogies in crystal field theory. In particular, a set of L^{σ} cluster orbitals should be split in the opposite sense to a set of l atomic orbitals on the central atom of a complex with ligands in the same arrangement as the cluster vertices.

In fact, there is another center-of-gravity rule that applies to complete sets of, e.g., σ and π cluster orbitals. If each orbital in an interacting set has the same self-energy, α, then one can easily prove that there is a center-of-gravity relative to $\alpha = 0$.

Acknowledgment. D.J.W. thanks Downing College Cambridge for financial support for his visit to Oxford, during which this work was performed, and Dr. D. W. Fowler for his borane coordinates.

Registry No. Borane, 13283-31-3.

Contribution from the Department of Chemistry, University of Chicago, 5735 South Ellis Avenue, Chicago, Illinois 60637, and Inorganic Chemistry Laboratory, University of Oxford, South Parks Road, Oxford OX1 3QR, United Kingdom

Skeletal Rearrangements in Clusters. 2.

David J. Wales,*[†] D. Michael P. Mingos,[‡] and Lin Zhenyang[‡]

Received January 23, 1989

In this paper, we continue a theoretical study of the rearrangements of cluster skeletal atoms with emphasis on the possible differences between transition-metal and main-group clusters. We show that the selection rules for orbital-symmetry-forbidden "TSH-forced" crossings, derived for main-group clusters using Stone's tensor surface harmonic (TSH) theory, should also be applicable to transition-metal clusters as long as the metal fragments are isolobal to B-H. We also discuss the feasibility of various single edge-cleavage mechanisms that were not previously considered for main-group clusters in part 1. Using TSH theory and polyhedral skeletal electron pair theory[1] electron-counting rules, especially for "capping" and "condensation" principles, we find that most of the new processes recently suggested in another study are probably unfavorable. Some alternative mechanisms are therefore suggested, with particular attention being paid to the new possibilities predicted for transition-metal clusters.

Introduction

The theoretical study of rearrangements in cluster compounds has recently been elegantly analyzed with use of Stone's tensor surface harmonic (TSH) theory.[2-6] The new approach, due to Wales and Stone[7] (part 1 in this series), enables some rearrangement processes that have an orbital crossing, and are therefore "forbidden" in the Woodward-Hoffmann sense,[8] to be identified very simply. The analysis in part 1 explained, in terms of TSH theory, why Lipscomb's diamond-square-diamond (DSD) process[9] (illustrated in Figure 1) should in principle be energetically favorable and identified some special cases where it is not. It was built partly upon King's topological considerations, which distinguish between inherently rigid clusters (containing no *degenerate* edges) and those for which one or more DSD processes are *topologically* feasible.[10] An edge is termed *degenerate* if a DSD process in which it is broken leads to a product with the same cluster skeletal geometry as the starting molecule.

The conclusion of part 1 was that transition states between *closo*-boranes or *closo*-carboranes with a single atom on a principal rotation axis of order three or more will generally have an orbital crossing and hence be high-energy processes.[11] The effect of lower symmetry environments, for example, when there is a single atom on a 2-fold axis, was also considered. In this case, the barrier to rearrangement may also be large, depending upon the splitting of the HOMO and LUMO, which form a degenerate pair of E symmetry when the principal axis is of higher order. Substituents around the critical face at which the DSD process occurs may help to lower the barrier by increasing the difference between the electronic environments in the local x and y directions, and hence increasing the HOMO-LUMO gap.[7]

Independently, Johnston and Mingos recognized that for *closo*-boranes, $B_nH_n^{2-}$, with $4p + 1$ atoms, i.e. $B_5H_5^{2-}$ and $B_9H_9^{2-}$, the single DSD process is symmetry forbidden because a mirror plane is retained throughout.[12] In contrast, single DSD processes in which only a C_2 symmetry element is conserved, e.g. for $B_8H_8^{2-}$, do not involve a crossing and are symmetry allowed. This symmetry rule has its origins in the nodal characteristics of L^{π} and $\bar{L}^{\pi}$ cluster orbitals and their behavior under the symmetry op-

[†] University of Chicago.
[‡] University of Oxford.

(1) Mingos, D. M. P. *Acc. Chem. Res.* **1984**, *17*, 311.
(2) Stone, A. J. *Mol. Phys.* **1980**, *41*, 1339.
(3) Stone, A. J. *Inorg. Chem.* **1981**, *20*, 563.
(4) Stone, A. J.; Alderton, M. J. *Inorg. Chem.* **1982**, *21*, 2297.
(5) Stone, A. J. *Polyhedron* **1985**, *3*, 1299.
(6) Stone, A. J.; Wales, D. J. *Mol. Phys.* **1987**, *61*, 747.
(7) Wales, D. J.; Stone, A. J. *Inorg. Chem.* **1987**, *26*, 3845.
(8) Woodward, R. B.; Hoffmann, R. *Angew. Chem., Int. Ed. Engl.* **1969**, *8*, 781.
(9) Lipscomb, W. N. *Science (Washington, D.C.)* **1966**, *153*, 373.
(10) King, R. B. *Inorg. Chim. Acta* **1981**, *49*, 237.
(11) Gimarc, B. M.; Ott, J. J. *Inorg. Chem.* **1986**, *25*, 83, 2708.
(12) Johnston, R. L.; Mingos, D. M. P. *Polyhedron*, in press.

0020-1669/89/1328-2754$01.50/0

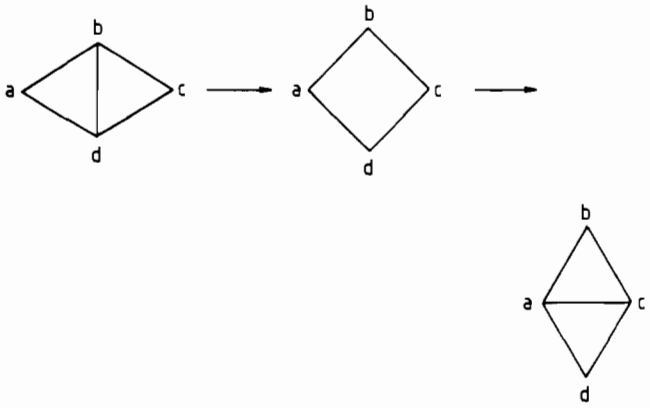

Figure 1. Diamond–square–diamond (DSD) process.

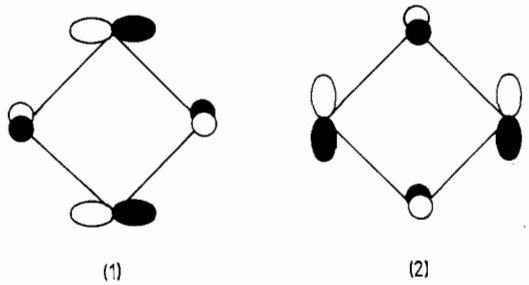

Figure 2. Frontier orbitals in the open face of the single DSD transition state. Both orbitals are antisymmetric with respect to a C_2 rotation about an axis through the center of the face. Under reflection in vertical and horizontal mirror planes, orbital 1 is antisymmetric and symmetric, respectively, while orbital 2 behaves in the opposite fashion.

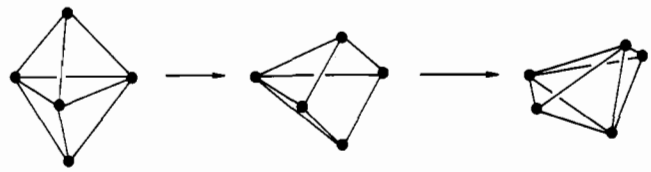

Figure 3. Single diamond–square–diamond process for $B_5H_5^{2-}$.

erations relevant to the DSD process.

Using the above rules, which are discussed in the following section, and the additional criterion that multiple DSD processes are likely to be less favorable than the single DSD process, it is possible to rationalize the whole range of rearrangement rates of the *closo*-boranes and *closo*-carboranes. In this paper, we will extend the analysis to discuss alternative rearrangements that have recently been proposed[13] and may be relevant to transition-metal clusters.

TSH Theory Symmetry-Forced Crossings

In the transition state for the single-DSD process (Figure 1), the frontier orbitals of the open face (Figure 2) are self-conjugate; i.e., they are related by a rotation of each p^π orbital component about the radius vector of the atom, all in the same sense. This relation is the TSH parity or pairing principle.[2] If the cluster has $4p + 1$ atoms ($p = 1, 2, \ldots$), these orbitals are degenerate, but otherwise they need not be. The symmetry selection rule developed in part 1 enables one to identify mechanisms where there must be an orbital crossing due to a degeneracy at the HOMO–LUMO level. An example of such a "forbidden" process is the single DSD process for $B_5H_5^{2-}$, where the "transition state" would have a single atom on a 4-fold principal axis (Figure 3).

A more detailed examination enables us to identify cases where there must be a crossing in lower point group symmetry. These are not so much forced by a degeneracy of the frontier orbitals in the prevailing point group symmetry but rather by the pairing principle causing a change in the number of occupied orbitals with a given parity under reflection. The TSH theory parity operation corresponds to the pseudoscalar irreducible representation of the point group that is symmetric to all proper rotations and antisymmetric to improper rotations and reflections. Therefore L^π and $\bar{L}^\pi$ orbitals related by the parity operation have opposite parities with respect to reflection. The high-symmetry case can also be discussed in terms of the parity under reflection argument, which proceeds as follows. The frontier orbitals in the transition state (Figure 2) have complementary characteristics with respect to reflection in any mirror planes that pass through the open square face. If the open face is squeezed along a mirror plane that is retained throughout the rearrangement, then the two parity-related orbitals are split apart. Squeezing across the same mirror plane, however, causes splittings of the two components in the opposite sense, and hence there is an orbital crossing in the correlation diagram (Figure 4). If a C_2 axis is retained during the DSD process then there is an avoided crossing because the frontier orbitals are both antisymmetric under this operation. In summary; *a DSD process in which a mirror plane is retained throughout involves an orbital crossing and is therefore "forbidden"*, in agreement with Gimarc and Ott's analysis.[11] This observation was alluded to in part 1 where we remarked that orbitals belonging to the L^π frontier set can only cross their $\bar{L}^\pi$ partners if an inversion center or σ_h mirror plane is retained throughout the rearrangement. Actually, this statement is incomplete because there are point groups where some of the irreducible representations (IRs) are self-conjugate under the parity operation and others are not. The point groups that may be conserved throughout actually fall into three distinct classes:[14] (1) L^π and $\bar{L}^\pi$ always transform according to different IRs. Groups of this type include the inversion and/or a σ_h mirror plane, e.g. C_i, C_s, C_{2v}, O_h, etc. (2) L^π and $\bar{L}^\pi$ always transform according to the same IRs. This is the case for point groups such as C_n and D_n where the parity operator transforms as A_1. (3) Some L^π and $\bar{L}^\pi$ transform in the same way while others do not. Groups of this type include C_{nv}, ($n \geq 3$), and S_{4n}. For a DSD process mirror planes or a C_2 axis may be conserved, and in the point groups C_s and C_2 the parity operator transforms as A″ and A, respectively. Hence, if a mirror plane is conserved, parity-related L^π and $\bar{L}^\pi$ always span different IR's (and can cross), while if a C_2 operation only is conserved, they must span the same IR (and cannot cross). We would also expect these results to extend to cases where the symmetry elements are only approximate, but in a less rigorous manner.

We may also apply this symmetry selection rule to nondegenerate rearrangements in which the starting and finishing clusters are different, but both have $n + 1$ skeletal electron pairs. For

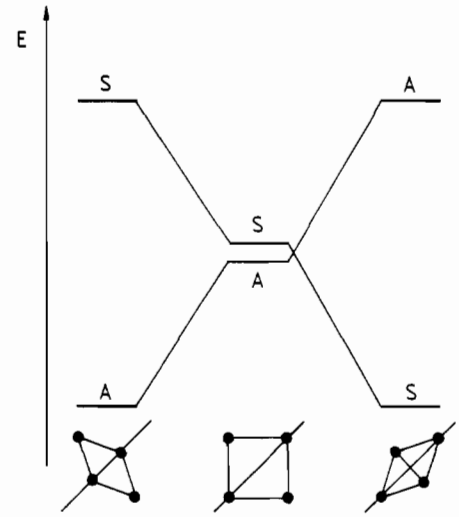

Figure 4. Orbital correlation diagram for a single DSD process in which a mirror plane through two of the critical atoms is retained throughout. An orbital crossing occurs due to the change in bonding character of the parity related orbitals.

(13) Rodger, A.; Johnson, B. F. G. *Polyhedron* **1988**, *7*, 1107.

(14) Fowler, P. W. *Polyhedron* **1985**, *4*, 2051.

example, in the single DSD process that interconverts 1,2-$C_2B_3H_5$ to 1,5-$C_2B_3H_5$, a mirror plane is retained throughout and there is a crossing.[11] In later sections, we will discuss some cases where the geometry change is far greater than in this example. The analysis may also be extended to multiple DSD processes, whether they be concerted or stepwise. For example, consider a degenerate, concerted double DSD process in which a mirror plane is preserved throughout and passes through both open faces in the transition state. If one edge is broken across the mirror plane and the other is broken simultaneously in the plane, then there is no orbital crossing. This follows because of the complementary nature of the frontier orbitals in the two open faces that preserves the total number of occupied orbitals with S and A parity under the reflection by means of two avoided crossings. In contrast, if two edges are broken and made parallel to one another (both in or both across the mirror plane), then the number of S or A parity orbitals in the occupied set changes by plus or minus two.

We will refer to crossings of the above type as "TSH theory symmetry forced" because they are derived from TSH theory. Clearly the identification of such processes is very important, as indicated by the success of the analysis in part 1. In a later section we show that the same rules can sometimes be applied to rearrangements of transition-metal clusters.

We should also explain why the degeneracies and crossings are predicted to occur at the HOMO–LUMO level. For a main group cluster the degenerate E-type pair are non-bonding with respect to the self-energy, α, of a valence-shell p orbital. Since the frontier orbitals of main group clusters generally consist of the π cluster orbitals, it follows that the degeneracy will occur at the HOMO–LUMO level and will therefore correspond to a crossing of an occupied and a virtual molecular orbital.

The orbital symmetry rules, above, can also be related to the electron-counting rules for closo, nido, and arachno clusters. The parent *closo*-deltahedra $B_5H_5^{2-}$ and $B_9H_9^{2-}$ are characterized by $n + 1$ skeletal bonding orbitals. The transition state for the single DSD process results in square-faced *nido*-deltahedra with C_{4v} symmetry, which are characterized by $n + 2$ skeletal electron pairs. The presence of the 4-fold rotation axis means that the frontier orbitals have E symmetry. Consequently, the single DSD process is unfavorable because the ground-state and transition-state geometries have different closed-shell requirements. They are forbidden by orbital symmetry considerations because the E pair at the HOMO–LUMO level corresponds to an orbital crossing.

In contrast, the corresponding single DSD process for $B_8H_8^{2-}$ probably leads to a bicapped trigonal-prismatic intermediate structure with C_{2v} symmetry. It has been demonstrated from the "capping principle"[15] that a bicapped trigonal prism can be associated with either 9 or 10 skeletal bonding molecular orbitals. Consequently, the starting and transition-state geometries have compatible closed-shell requirements and are not anticipated to have very different energies. Furthermore, there is no 3-fold or higher principal rotation axis in the transition state, and no mirror plane is maintained throughout—hence, there should be no orbital crossing.

The following geometric and electronic criteria can therefore be used as a basis for predicting the relative activation energies for skeletal rearrangements in main-group clusters: (1) Symmetry-allowed single DSD rearrangements will have the lowest activation energies. (2) Multiple DSD processes are only expected to be favorable if they are allowed by orbital symmetry considerations and involve intermediates with compatible closed-shell requirements. This idea will be further developed below; it may be applied to multiple DSD processes whether they are considered to be concerted or stepwise. (3) Processes that generate a new geometry with incompatible closed-shell requirements will have higher activation energies. (4) Single DSD processes that involve a TSH forced crossing are expected to be somewhat less favorable than mechanisms belonging to category 3. (5) Multiple DSD processes involving incompatible closed-shell requirements or TSH forced crossings will be the least favorable of all.

(15) Forsyth, M. J.; Mingos, D. M. P. *J. Chem. Soc., Perkin Trans.* **1977**, 610.

Single Edge-Cleavage Processes

Recently Rodger and Johnson have considered the geometrical symmetry selection rules for the rearrangement of transition-metal clusters with between 5 and 12 atoms.[13] Their approach must be carefully distinguished from the present work, as it is not concerned with the conservation of *orbital* symmetry, but with the fact that any reaction mechanism must follow a vibrational normal mode of the cluster at every point. They consider single edge-cleavage processes only, on the grounds that these are expected to be most favorable. Some of these mechanisms correspond to the diamond–square–diamond processes considered previously,[7] except that they are considered to be stepwise if more than one edge must be broken. In fact, all of the processes considered in part 1 are geometrically allowed. The relationship between the geometric and orbital symmetry selection rules will be discussed in more detail in part 3 of this series.[16]

More interesting are the mechanisms that were not considered for main-group clusters because they involve tetrahedral caps in the intermediate structures. Such geometries were discounted for main-group clusters because they are rarely observed in solid-state structural analyses. For transition-metal clusters, however, such structures might play a more significant role. Incidentally, the fact that all the rearrangement rates of the boranes and carboranes could be rationalized in terms of DSD processes provides circumstantial evidence that the other structures, to be considered below, are too high in energy to play any part for these species.

In the following sections, we will consider all the single edge-cleavage mechanisms suggested by Rodger and Johnson that have not already been discussed in part 1, as well as some alternative possibilities. In general, these could be written as multiple DSD processes too, but it seems much more likely from the present work that they would be stepwise, especially when more than two edges must be broken. Since these processes do not lead immediately back to the original geometry, we must be more careful in applying the TSH-forced crossing rules. Some new criteria, alluded to in category 2 in the previous section, will also be developed in terms of the usual electron counting rules for closo, nido, and arachno clusters, plus the "capping"[17–19] and "condensation"[20] principles. Here the discussion is no longer limited to main-group clusters.

The electron-counting rules determine whether the predicted electron count changes from the starting cluster to the suggested intermediate. Processes where the electron count changes are expected to be relatively unfavorable because there will be an unoccupied low-lying orbital or an occupied high-lying orbital. For example, if a DSD process converts a *closo*-deltahedron into a capped deltahedron with $n - 1$ vertices and a principal rotation axis of order three or more passing through the cap, then the process will probably be unfavorable. This is because capped deltahedra of this type have a nonbonding L^π $\bar{L}^\pi$ E pair and n skeletal bonding orbitals.[7] The electronic ground state of such a species would be a triplet and subject to a Jahn–Teller distortion.[21] In any case the frontier orbitals are high lying because they are nonbonding. For DSD processes that result in a capped deltahedron with lower symmetry, the "E" pair is split, but we still expect the orbitals to be approximately nonbonding and the HOMO in particular to be high lying.[7] A low-energy pathway between such structures therefore appears unlikely.

Note, however, that this "skeletal electron count selection" (SECS) rule should not be placed upon the same footing as the orbital symmetry or geometrical symmetry selection rules above. It would be quite wrong to describe mechanisms in which the predicted electron count changes as "forbidden", and we will not do so. Nonetheless, we would still expect them to be relatively

(16) Wales, D. J.; Mingos, D. M. P. *Polyhedron*, in press.
(17) Mingos, D. M. P. *Nature, Phys. Sci.* **1972**, *236*, 99.
(18) Mason, R.; Thomas, K. M.; Mingos, D. M. P. *J. Am. Chem. Soc.* **1973**, *95*, 3802.
(19) Mingos, D. M. P. *J. Chem. Soc., Dalton Trans.* **1977**, 610.
(20) Mingos, D. M. P. *J. Chem. Soc., Chem. Commun.* **1983**, 706.
(21) McIvor, J. W.; Stanton, R. E. *J. Am. Chem. Soc.* **1972**, *94*, 8618. McIvor, J. W.; Stanton, R. E. *J. Am. Chem. Soc.* **1975**, *97*, 3632.

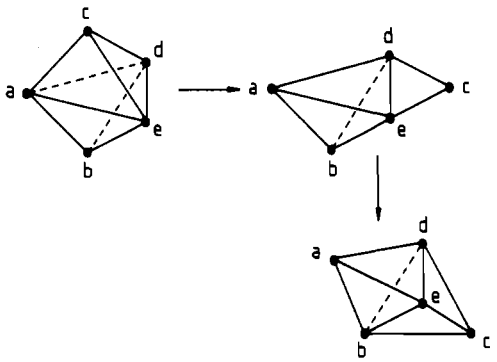

Figure 5. Edge-bridging process for a trigonal bipyramid.

high activation energy processes, and predictions will be made on the basis of this assumption.

Five-Atom Clusters

For the trigonal bipyramid the single diamond–square–diamond process is forbidden by the TSH-forced crossing rule (criterion 4 of the previous section), as described in part 1. Note that a mirror plane passing through the critical face is retained throughout this process. The alternative edge-bridging mechanism was also considered in part 1; it leads to an edge-bridged tetrahedral "transition state" as illustrated in Figure 5. In this geometry, there is a single atom on a 2-fold rotation axis, and there can be no TSH forced crossing. (Although the process retains a mirror plane, it does not correspond to a DSD rearrangement.) The actual energy barrier will depend on how widely the two components of the idealized "E" pair are split.

This can also be viewed in tems of the "condensation rules", which state that an edge bridge will increase the total electron count by one electron pair,[22] which corresponds to the higher lying of the idealized "E" pair in the alternative description. Furthermore, it does not seem possible to rearrange the ligands so as to make this extra orbital inaccessible. The presence of an unoccupied low-lying orbital may not always result in a prohibitively large energy barrier, but in this case it is associated with a high-lying HOMO that corresponds to the lower lying component of the idealized "E" pair (Figure 6a). If the cluster were very large, however, the barrier to the edge-bridging process might be reduced by the three-center interaction illustrated in Figure 6b. From this point of view, the trigonal-bipyramid represents the worst possible case for this mechanism. Also note that the number of skeletal electron pairs remains constant at six for both the trigonal bipyramid and the tetrahedron. In general, if we start from an *n*-vertex *closo*-deltahedron with a tetrahedral cap, we would expect the number of skeletal electron pairs to remain unchanged at *n* for the edge-bridged *closo*-deltahedral geometry (rather than $n + 1$ in this case).

Six-Atom Clusters

For the octahedron, there is no degenerate single DSD process possible, and we must consider intermediates with alternative geometries. The single DSD-type process, illustrated in Figure 7, leads from the octahedron to the bicapped tetrahedron. In this case, the number of skeletal electron pairs decreases from seven to six (using the capping principle), and one skeletal electron pair must reside in a high-lying orbital if the electron count is to be conserved. Furthermore, a mirror plane through the critical face is conserved. Hence, we would expect this process to be unfavorable. Also note that the bicapped tetrahedron can be viewed as an "electron-precise" cluster (i.e. edge-bonded), while the bonding in the octahedron must be rationalized in delocalized terms. Since the DSD process does not change the number of edges in a cluster, it follows that *the skeletal electron count must change if the skeleton is converted from one associated with an "electron-precise" count to one involving delocalized bonding* (or vice versa). Some alternative mechanisms involving the rupture

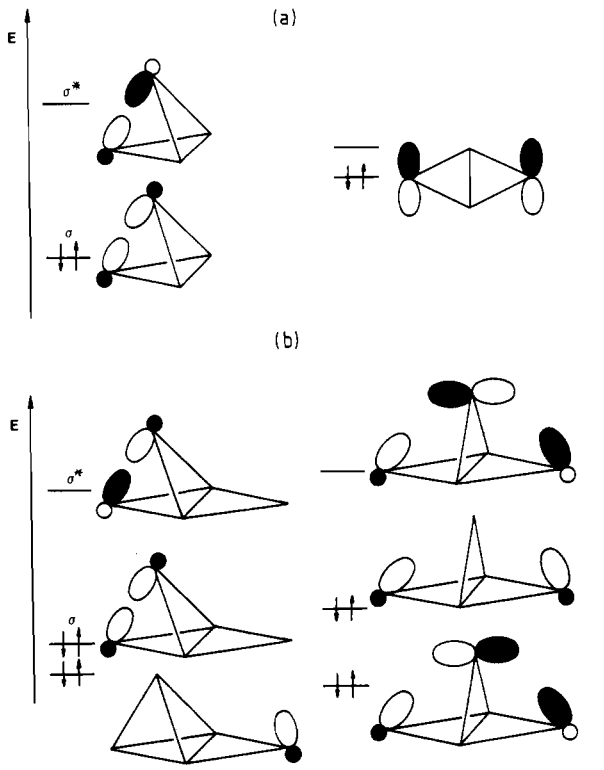

Figure 6. Energy level diagrams for the frontier orbitals in an edge-bridging rearrangement. (a) In a small cluster the idealized "E" pair lie close together, and there is a large barrier. (b) In a hypothetical large cluster, a three-center interaction may be possible, which would lower this barrier.

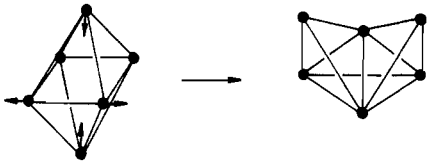

Figure 7. Edge-cleavage, edge-formation process leading from the octahedron to the bicapped tetrahedron. The expected number of skeletal electron pairs changes from 7 to 6.

of more than one edge at a time are discussed for transition-metal clusters in a later section.

An alternative possibility is the trigonal-twist mechanism in which the two triangles of atoms rotate relative to one another to give a trigonal-prismatic intermediate. The molecular orbitals for the octahedron and the trigonal prism have been analyzed elsewhere,[23] and the relevant correlation diagram is given in Figure 8. Between the octahedron and the trigonal prism, the cluster has D_3 symmetry, and the e_g component of t_{2g} and the e_u component of t_{2u} both transform as e. These evolve into e″ and e′ in the trigonal prism by means of an avoided crossing. A second avoided crossing is involved in the rearrangement from the trigonal prism to the new octahedron. The rearrangement from an octahedral cluster involving delocalized skeletal bonding to the trigonal prism, which may usually be described in terms of edge-localized bonding, clearly involves a large energy barrier. The increment in the number of skeletal electron pairs from seven to nine in the "transition state" contributes to the high barrier. In a later section, we shall give an example of a platinum cluster where the barrier to an analogous rearrangement is small.

We also note that McKee[24] has recently investigated some relatively high-energy "local bond rotation" mechanisms for octahedral $C_2B_4H_6$. In fact, these can be considered as concerted double DSD processes in which at most a C_2 axis is retained throughout, and they are therefore orbitally allowed. Furthermore,

(22) McPartlin, M.; Mingos, D. M. P. *Polyhedron* **1984**, *3*, 1321.

(23) Johnston, R. L.; Mingos, D. M. P. *J. Organomet. Chem.* **1985**, *280*, 407.

(24) McKee, M. L. *J. Am. Chem. Soc.* **1988**, *110*, 5317.

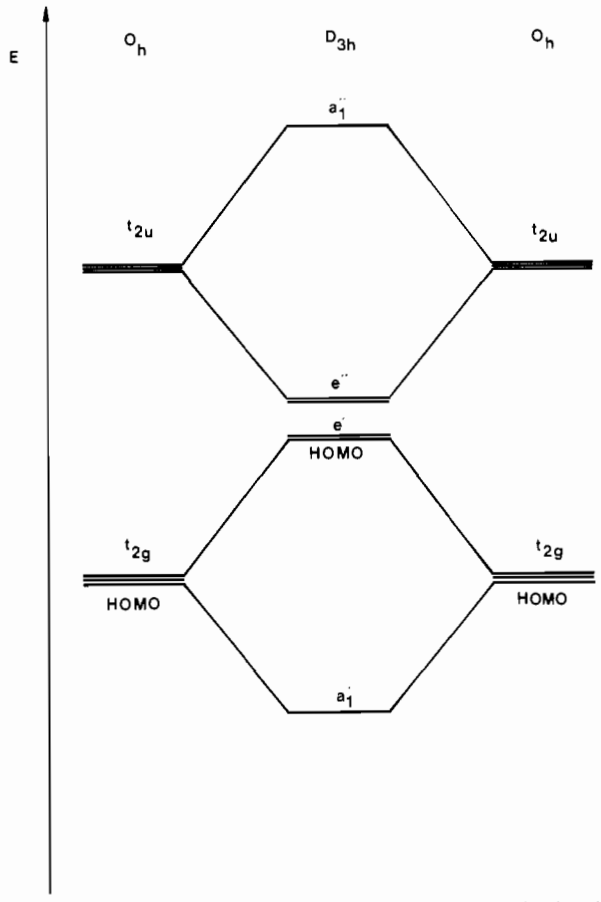

Figure 8. Correlation diagram for the trigonal-twist mechanism in a main-group cluster.

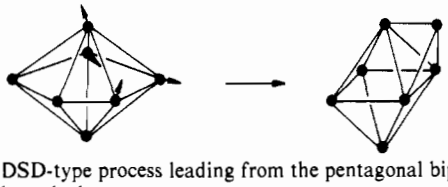

Figure 9. DSD-type process leading from the pentagonal bipyramid to the capped octahedron.

the crossing in McKee's reaction scheme for the conversion of 1,6-$C_2B_4H_6$ into 1,2-$C_2B_4H_6$ also fits in with the present work, as two mirror planes through a critical face are retained.

Seven-Atom Clusters

Now consider the pentagonal bipyramid. Performing a DSD process in which an equatorial edge is broken actually leads to little change in the structure (remember that all the edges are notional), so we will only consider the mechanism illustrated in Figure 9 in which a capped octahedron is produced. A second DSD process (55(34) in King's notation) would give a permutation of the starting geometry. In the first single DSD process, a mirror plane through the critical face is retained throughout and the capped octahedron has a single atom on the principal 3-fold rotation axis. Hence, there is a nonbonding e pair as well as seven skeletal bonding orbitals. Alternatively, from the capping principle, the number of skeletal electron pairs is predicted to decrease from eight to seven, and the additional electron pair would therefore have to occupy the nonbonding e pair of orbitals. The concerted double DSD does not involve a crossing, but the open faces would have to share an edge. Hence, neither a concerted nor a stepwise mechanism is expected to be as favorable as the double DSD for the nine-atom tricapped trigonal prism considered below.

We now deduce a further generalization concerning mechanisms that generate structures with tetrahedral chambers. Consider the process

n-vertex deltahedron → $(n - 1)$-vertex deltahedron plus cap

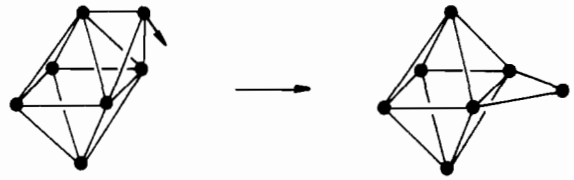

Figure 10. Edge-bridging mechanism for the capped octahedron.

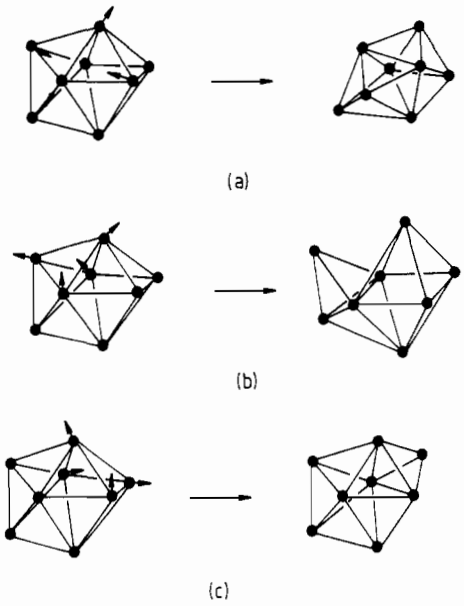

Figure 11. DSD processes for the eight-atom dodecahedron. In King's notation they are (a) 55(44), (b) 54(55), and (c) 54(54).

The skeletal electron count for this process changes from $n + 1$ to n, assuming that the starting geometry is not subject to a symmetry-determined deviation from the usual $n + 1$ skeletal orbitals.[14] Since none of the usual *closo*-deltahedral geometries for clusters with 5–12 vertices deviate from the $n + 1$ rule, it follows that *none of them are expected to readily undergo a rearrangement that proceeds through a structure with a tetrahedral cap.*

If we start from the capped octahedral geometry, then an edge-bridging process is possible that leads to an equivalent capped octahedral geometry via an edge-bridging "transition state", as illustrated in Figure 10. The considerations which were discussed above for five-atom clusters indicate that this process, which is not symmetry forbidden, may be somewhat more favorable for the larger species, but it is still expected to have a significant energy barrier due to the single atom on the 2-fold rotation axis. Although such a process is unfavorable for main-group clusters, we see later that it may be favorable for some transition-metal clusters with d^{10} capping atoms.

Eight-Atom Clusters

Three possible DSD processes are illustrated for the eight-atom dodecahedron in Figure 11. In King's notation[10] they are designated as 55(44), 54(55), and 45(45) for parts a–c, respectively, of Figure 11. (For an $\alpha\beta(\gamma\delta)$ process, an edge is broken between two vertices of connectivity α and β, and an edge is made between two vertices of connectivity γ and δ, which are the two common nearest neighbors of the first two vertices in the starting geometry.) The first of the above mechanisms is the simple DSD process in which a degenerate edge is broken—it leads back to the starting geometry. The only symmetry element retained throughout is a C_2 axis. Since this process is allowed by the orbital selection rules, it is most unlikely that either of the other suggested mechanisms plays any significant part in the rearrangement of dodecahedral clusters. Furthermore, both these alternative processes are expected to lead to changes in the skeletal electron count. For the 54(55) mechanism (Figure 11b) the resulting cluster may be described as an octahedron and a trigonal bipyramid sharing

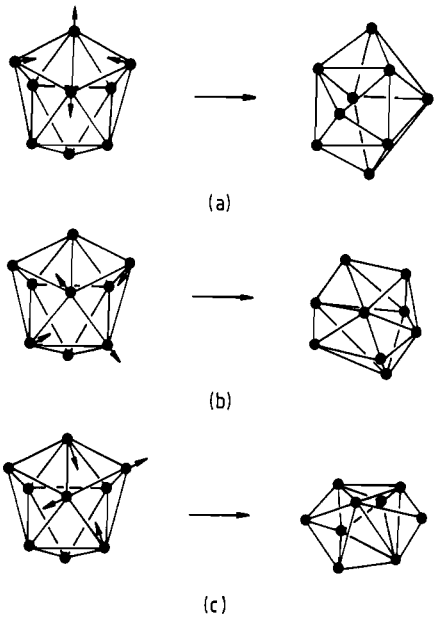

Figure 12. DSD processes for the tricapped trigonal prism. In King's notation they are (a) 55(44), (b) 55(54), and (c) 54(55).

a face. The condensation principle predicts that this species should have 10 skeletal electron pairs: one more than the starting geometry. For the 45(45) process (Figure 11c), a capped pentagonal bipyramid results, and we predict a decrease in the skeletal electron pair count from nine to eight.

Nine-Atom Clusters

For the tricapped trigonal prism, we again consider three possible edge-cleavage processes: 55(44) (Figure 12a), 55(54) (Figure 12b), and 54(55) (Figure 12c). The first of these corresponds to the symmetry-forbidden single DSD mechanism which has a TSH forced crossing.[7] The second process (Figure 12b) is also symmetry forbidden since a mirror plane is conserved, and results in a deltahedral cluster with no tetrahedral chambers. A further 65(44) DSD process leads back to the tricapped trigonal prism. The two-step concerted process is symmetry allowed, since the critical edges involved are mutually perpendicular relative to the conserved mirror plane.[11] The third process (Figure 12c) leads to a capped eight-atom dodecahedron, and a reduction in the number of skeletal electron pairs from 10 to 9 is expected. The double DSD process is likely to be the most favorable, as per the analysis in part 1.

Ten-Atom Clusters

The 10-vertex deltahedron has three distinct edges, and the three DSD processes that correspond to breaking these edges are illustrated in Figure 13. First, consider the 55(45) edge-cleavage shown in Figure 13a. A subsequent 65(44) single DSD process involving any of the three equivalent edges connected to the six-coordinate atom on the 3-fold principal axis leads us back to the starting skeleton. This represents a double DSD mechanism that was not considered in part 1. First, note that the intermediate structure has a single atom on the 3-fold axis and that a mirror plane is retained through the critical face, as for the capped octahedron above. Hence, we expect there to be a significant energy barrier to the stepwise process. A concerted double DSD would require the two square faces to share an edge—there is no forced orbital crossing as no mirror plane is conserved. Hence, $B_{10}H_{10}^{2-}$, like $B_9H_9^{2-}$, has a symmetry-allowed concerted double DSD. The fact that three carborane isomers are known for $C_2B_8H_{10}$ and only one for $C_2B_7H_9$ may indicate that the concerted double DSD for the nine-vertex species is more favorable, presumably because the two square faces share only a single vertex, rather than an edge.

The 55(55) process (Figure 13b) leads to a rather strained deltahedral structure with two six-coordinate vertices, but with no tetrahedral caps. Four steps, corresponding to the quadruple

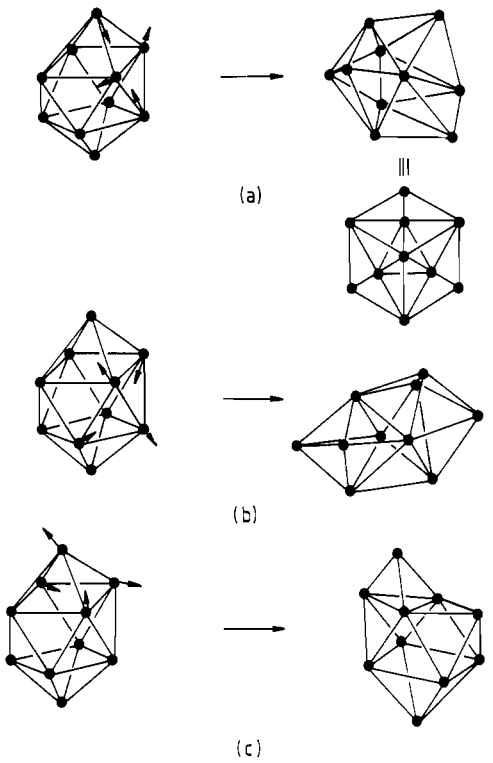

Figure 13. DSD processes for the 10-vertex deltahedron. In King's notation they are (a) 55(45), (b) 55(55), and (c) 54(55).

DSD mechanism discussed previously,[7] are required to produce a permutation of the vertices of the starting material.

In the 54(55) process, a tricapped trigonal prism with an additional tetrahedral cap is produced, and the skeletal electron count is reduced from 11 to 10 pairs. As mentioned above, any DSD process that changes a *closo*-deltahedral geometry into a closo structure with a tetrahedral chamber is expected to reduce the skeletal electron pair count and be relatively unfavorable. Any process in which an edge connected to a four-coordinate vertex is broken will produce a tetrahedral chamber, so that any DSD mechanism that can be written as $\alpha 4(\beta\gamma)$ is expected to be unfavorable if the starting geometry has no tetrahedral caps itself.

Eleven-Vertex Clusters

For the 11-vertex deltahedron, there are a number of possible single edge-cleavage processes, several of which do not produce any tetrahedral chambers. Since there is a symmetry-allowed single DSD, in which there is no mirror plane preserved throughout, it does not seem worthwhile analyzing the alternative mechanisms, as they are not expected to have a significant role to play in the chemistry of such molecules.

Twelve-Vertex Clusters

For the 12-vertex icosahedron all 30 edges are, of course, equivalent. The icosahedron represents an interesting case because in part 1 we showed that both the previously proposed transition states, corresponding to concerted pentuple and sextuple DSD mechanisms, are not true transition states at all. Furthermore, since rearrangement of the carborane isomers $C_2B_{10}H_{12}$ is only achieved at relatively high temperatures, we would not expect there to be a favorable low-energy pathway comparable to the single DSD process in $B_8H_8^{2-}$. In the 55(55) process (Figure 14a) two mirror planes through the critical face are conserved throughout and there should be an orbital crossing. A series of six stepwise DSD processes, in which the bold edges in Figure 14b are broken, corresponds to the concerted sextuple DSD mechanism. In King's notation,[10] the most symmetrical sequence is 55(55), 65(55), 65(45), 65(44), 66(44), in which only three distinct intermediate geometries are involved. The first is illustrated in Figure 14; it also appears after step five in this sequence. The second, which also appears after step four, is shown in Figure 14c, and the third is the fascinating D_{3h} structure of Figure 14d. Steps two, five,

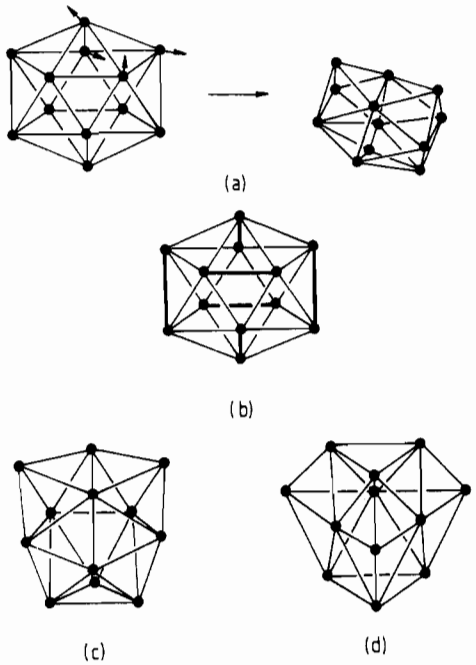

Figure 14. (a) Unique single DSD process for the 12-vertex icosahedron. (b) Edges that must be broken in the stepwise sextuple DSD mechanism. (c) Structure that appears after steps two and four of the stepwise sextuple DSD mechanism. (d) D_{3h} geometry that appears after step three of the stepwise sextuple DSD mechanism.

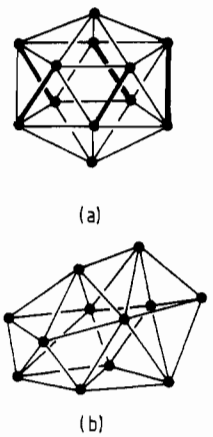

Figure 15. (a) Edges that must be broken in the stepwise pentuple DSD mechanism. (b) Structure that appears after steps two and three of the stepwise pentuple DSD mechanism.

and six of this sequence should also involve orbital crossings because mirror planes are conserved, so a less symmetrical series of steps may be more favorable. None of the above intermediate species appear to be present in the tabulation of 12-vertex forms due to Fuller and Kepert.[25,26] There is an interesting correspondence between this stepwise sextuple DSD sequence and the six-step notional rearrangement proposed for the truncated icosahedral C_{60} molecule.[27] In the latter case, the rearrangements interchange five- and six-membered rings; the isomorphism is clearly due to the point group symmetry.

The bold edges in Figure 15a indicate a stepwise sequence of DSD processes corresponding to the concerted pentuple DSD mechanism. Only two distinct structures are encountered in the sequence 55(55), 65(54), 65(54), 65(54), 66(44). The first, which appears after steps one and four, is illustrated in Figure 14a, and the second, which appears after steps two and three, is shown in Figure 15b. The first and last steps should involve orbital crossings because two mirror planes through the critical face are conserved throughout.

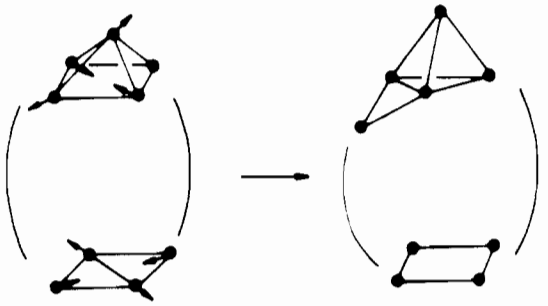

Figure 16. Formation of a nido cluster plus tetrahedral cap from a (highly schematic) general deltrahedron.

Although this sequence contains fewer steps than the stepwise sextuple DSD mechanism, the structure encountered after steps two and three is very "flat" and very distorted from a spherical geometry (this is best seen from models). The experimental evidence for the interconversion of the carborane isomers $C_2B_{10}H_{12}$ indicates that the permutation corresponding to the sextuple DSD process occurs more easily than the permutation corresponding to the pentuple DSD, although both have significant activation energy barriers. Furthermore, from the calculations performed in part 1, it seems likely that the rearrangements are indeed stepwise. It may be that the distorted structure encountered in the five-step path (Figure 15b) is responsible for the different rates observed. The high temperatures required to achieve both rearrangements testify to the forbidden nature of some of the steps, and there is no low-energy pathway in either case, concerted or stepwise.

Alternative Mechanisms

In the previous section we concluded that the only favorable single edge-cleavage DSD-type processes for *closo*-deltahedral clusters of between 5 and 12 atoms are those previously considered in part 1. This being the case, we will widen the scope of this study to enquire as to the feasibility of some alternative mechanisms. There are several new possibilities for transition-metal clusters that find no counterparts in main-group cluster chemistry. First, there are many transition-metal clusters for which there are no isostructural boranes or carboranes. Second, the metal fragments may be able to vary the number of electrons and orbitals that are contributed to skeletal bonding by changes in geometry, and so stabilize otherwise high-energy structures. Such behavior is most likely for metal–ligand combinations that are able to form both 16- and 18-electron complexes, such as nickel, palladium, and platinum. Third, there are metals such as gold and platinum that form clusters which have a quite different pattern of skeletal molecular orbitals from those found in borane clusters. Consequently the TSH forced-crossing rule will no longer be applicable. Examples of such behavior are given in the following sections. First, we suggest some more general alternative rearrangement mechanisms.

We have already noted that the edge-bridging mechanism[28] is unlikely to be very favorable, especially for smaller clusters. Johnson's "cap-extrusion" process[28] is also unlikely to be generally competitive, as the first step involves the formation of a tetrahedral cap that will lead to a decrease in the number of skeletal electron pairs.

As an alternative we suggest the following process, which is constructed so as to conserve the skeletal electron count:

n-vertex *closo*-deltahedron →
(n − 1)-vertex *nido*-deltahedron + tetrahedral cap

Similarly, the formation of an arachno cluster plus two tetrahedral caps would also be expected to conserve the electron count, but involves a greater structural perturbation than the above process,

(25) Fuller, D. J.; Kepert, D. L. *Inorg. Chem.* **1982**, *21*, 163.
(26) Fuller, D. J.; Kepert, D. L. *Polyhedron* **1983**, *2*, 749.
(27) Stone, A. J.; Wales, D. J. *Chem. Phys. Lett.* **1986**, *128*, 501.
(28) Johnson, B. F. G. *J. Chem. Soc., Chem. Commun.* **1986**, 27.

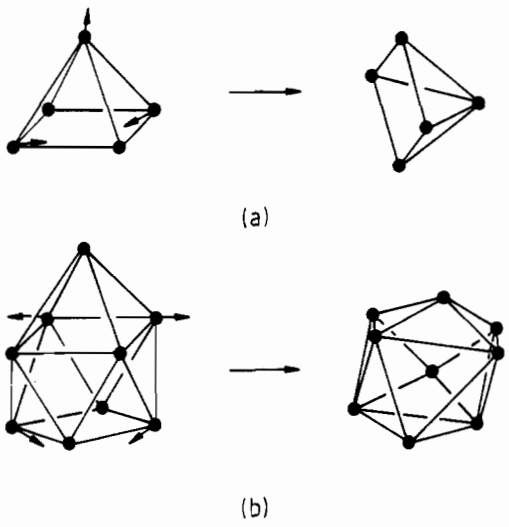

Figure 17. Square → diamond, diamond → square (SDDS) mechanism for (a) a square-based pyramid, and (b) a capped square antiprism.

which is illustrated in Figure 16.

Another possibility is a "pop-in, pop-out" mechanism where a tetrahedral cap at one site is subsumed back into the cluster skeleton, while another appears elsewhere. However, the considerable disruption to the cluster required for such a collective process probably makes it uncompetitive for clusters in the size range considered here.

Finally, the presence of a single square face in an otherwise deltahedral cluster opens up the possibility of an alternative low-energy rearrangement mechanism. Such a process may be written as a square → diamond, diamond → square or SDDS mechanism. This concerted process is illustrated for the square-based pyramid and the capped square antiprism in parts a and b of Figure 17, respectively. If a mirror plane is retained throughout, then this mechanism involves two orbital crossings if one edge lies in the mirror plane and the other lies across it. If the edges are parallel, as in Figure 17, then there are two avoided crossings and the process is orbital symmetry allowed. A Fenske–Hall[29] correlation diagram for *nido*-$B_9H_9^{4-}$ in the latter geometry is given in Figure 18. There is no TSH symmetry-forced crossing in this case, since the starting and finishing molecules both have a single atom on the 4-fold principle axis. Hence, this is expected to be a favorable process for nido transition-metal clusters. For *nido*-boranes, however, the presence of bridging hydrogen atoms around the open face means that this mechanism would involve a much greater perturbation to the structure of the cluster and is therefore not likely to occur. It could, however, be significant in accounting for the structures proposed for $B_8H_8^{2-}$ in solution,[30] where a fluxional bicapped-trigonal-prismatic geometry may be present. The SDDS mechanism is symmetry allowed for the latter species and may account for its nonrigidity. The same is also true for other species with no edge-bridging protons such as *nido*-$C_5H_5^+$ (square-based pyramid).[31]

Transition-Metal Clusters Conforming to the PSEPT

In transition-metal clusters the description of the frontier orbitals is more complicated than for main-group clusters, and we usually find that an S^σ cluster orbital is the HOMO, with a set of even π cluster orbitals lying below it.[32,33] The inwardly hybridized skeletal orbitals of π symmetry (with a nodal plane containing the radius vector of the skeletal atom from the center of the cluster) are now d and p in character. Hence, the predicted degeneracy for a system with a single atom on a principal axis

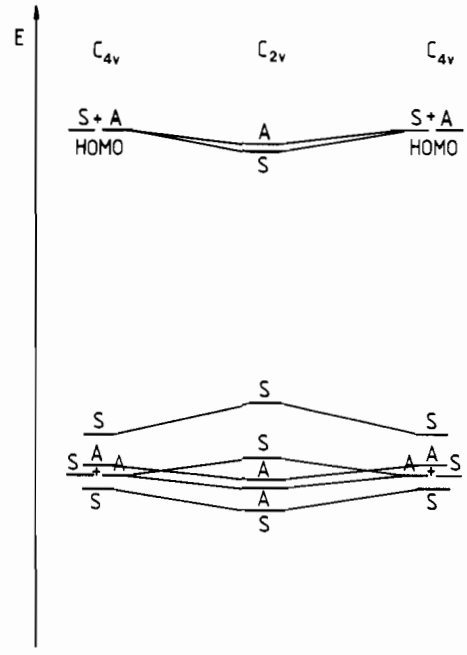

Figure 18. Fenske–Hall orbital correlation diagram for the SDDS process in *nido*-$B_9H_9^{2-}$. The labels S and A denote the parity of the orbitals with respect to reflection in the mirror plane, which is retained throughout this process.

of order three or more will not necessarily occur at the HOMO–LUMO level of the cluster. However, the crossover still represents a crossing between an occupied and a virtual molecular orbital and is therefore still expected to lead to a significant energy barrier.

Hence, we reach the conclusion that the symmetry selection rules developed for main-group clusters are expected to be applicable to rearrangements of transition-metal clusters, provided that the following points are true. (a) The ligands do not greatly reduce the energy barrier by lowering the symmetry. (b) The metal fragments remain isolobal with BH throughout the rearrangement process. (c) The metal cluster has a spectrum of skeletal molecular orbitals similar to those for the isostructural main group cluster. It should be noted, however, that since the splittings between L_{dp}^{π} and $\bar{L}_{dp}^{\pi}$ orbitals are much smaller for transition-metal than for main-group π orbitals the difference in activation energies between "allowed" and "forbidden" processes is correspondingly less. The additional criterion that multiple DSD processes will generally be less favorable than a single DSD process is also expected to hold. In metal carbonyl clusters where there are bridging ligands that lower the symmetry of the cluster, the symmetry rules are weakened and lower barriers for "forbidden" rearrangement processes are anticipated.

Low nuclearity (four to eight) metal atom clusters based on conical $M(CO)_3$ fragments, such as $[Os(CO)_3]_m$, are generally observed to be stereochemically rigid on the NMR time scale. Presumably in such clusters the spectra of skeletal molecular orbitals based on the outpointing dp hybrids of the conical $M(CO)_3$ fragments resemble those of boranes sufficiently for the arguments developed above to be applicable. For example, ^{13}C NMR evidence indicates that $Os_6(CO)_{18}$ (a bicapped tetrahedron), $Os_7(CO)_{21}$ (a capped octahedron), and $Os_8(CO)_{23}$ (a bicapped octahedron) are stereochemically rigid on the NMR time scale.[34] There is some evidence, however, that the barriers to rearrangement are lower than those in deltahedral boranes that have only orbital symmetry-forbidden DSD processes available. For example, $Os_6(CO)_{16}(P(OMe)_3)_2$ can be isolated in the solid state in two isomeric forms, based upon a bicapped tetrahedron, with the phosphites occupying either one or both of the capping atoms. In solution, the clusters exhibit NMR spectra consistent with this solid-state data with no fluxionality observed. However, when

(29) Hall, M. B.; Fenske, R. F. *Inorg. Chem.* **1972**, *11*, 768.
(30) Muetterties, E. L.; Wiersema, R. J.; Hawthorne, M. F. *J. Am. Chem. Soc.* **1973**, *95*, 7520.
(31) Stohrer, W.-D.; Hoffmann, R. *J. Am. Chem. Soc.* **1972**, *94*, 1661.
(32) Evans, D. G. *Inorg. Chem.* **1986**, *25*, 4602.
(33) Woolley, R. G. *Inorg. Chem.* **1987**, *27*, 430.
(34) Lewis, J.; Johnson, B. F. G.; et al. *J. Chem. Soc., Dalton Trans.* **1988**, 149.

the solution is allowed to stand, the more stable isomer is obtained.[34]

When asymmetry is introduced into the cluster by changing some of the metal atoms or replacing carbonyl ligands with, e.g. hydrides, the orbital symmetry rules begin to lose their validity. For example, the clusters $FeOs_nRu_{3-n}(\mu_2\text{-}H)_2(CO)_{13}$ (n = 0, 1, or 2) have distorted tetrahedral geometries. NMR data indicate that the isomers interconvert via a subtle "breathing" motion of the framework with concomitant movements of the carbonyls and hydrides.[35]

For higher nuclearity carbonyl clusters with combinations of bridging and terminal carbonyls, the situation is again less clear-cut because the bridging carbonyls interact strongly with the L^{π}_{dp} skeletal molecular orbitals. The great majority of pseudospherical deltahedral rhodium clusters, such as $Rh_6(CO)_{16}$ (octahedral), $Rh_7(CO)_{16}^{3-}$ (capped octahedral), $Rh_{13}H_{5-n}(CO)_{24}^{n-}$ (n = 1–4; cubotcahedral) and $Rh_{14}H_{4-n}(CO)_{24}^{n-}$ (capped cuboctahedral), are stereochemically rigid on the NMR time scale.[36]

In the distorted icosahedral cluster $Rh_{12}Sb(CO)_{27}^{3-}$, which has an interstitial antimony atom, the ^{13}C NMR data suggest that all the rhodium atoms are equivalent at ambient temperatures. A cuboctahedral intermediate has been proposed to account for this observation, but the present studies suggest that a fluxional process involving the carbonyls alone is more likely to be responsible.[37] The bicapped-square-antiprismatic clusters $Rh_{10}E(CO)_{22}^{n-}$ (n = 3, E = P or As; n = 2, E = S), which also have interstitial atoms, provide the only well-established examples of metal cluster compounds that are isostructural to *closo*-borane skeletal geometries and are stereochemically nonrigid. The NMR data in the range 90–100 °C indicate that a skeletal rearrangement is occurring in addition to the lower energy carbonyl permutations. Since the corresponding $B_{10}H_{10}^{2-}$ molecule is nonfluxional on the NMR time scale in this temperature range, it is probable that the double DSD process has a lower activation energy for the transition-metal clusters.[37,38]

In summary, although low-symmetry environments created by ligands may lead to a decrease in the activation energy barriers to rearrangements that are "forbidden" by orbital symmetry under high symmetry, the remaining barriers are still significant. Fluxional behavior is generally observed only at temperatures significantly above ambient temperature.

The related nido clusters $Rh_9E(CO)_{21}^{2-}$ (E = P or As), which have capped-square-antiprismatic geometries, become fluxional at room temperature,[39] indicating a somewhat smaller activation energy. The SDDS process, described above, may account for this behavior, and is illustrated in Figure 17b. There is no TSH symmetry-forced crossing.

Radially Bonded Metal Clusters

In some clusters, classified as "radially" bonded by Mingos,[40] the inwardly hybridized tangential p^{π} orbitals are too high in energy to contribute any accessible skeletal orbitals. In such clusters, the TSH forced-crossing rule is inapplicable because it assumes that all the even π cluster orbitals are occupied. In these radially bonded clusters, the number of skeletal bonding orbitals remains constant so long as all the skeletal atoms remain roughly disposed over the surface of a sphere.[41]

All three-dimensional gold clusters $Au(AuPR_3)_n^{x+}$ (n = 7–12) have a set of four radial skeletal bonding orbitals consisting of S^{σ}, P^{σ}_x, P^{σ}_y, and P^{σ}_z. Any rearrangement that proceeds along a pathway in which a roughly spherical topology is maintained is symmetry allowed, because the molecular orbitals constitute a complete spherical set and therefore correlate smoothly. Furthermore, since the Au–Au radial bonding is stronger than the tangential bonding, the energy differences between alternative cluster geometries is small, and these compounds are expected to be stereochemically nonrigid. There is a significant amount of ^{31}P NMR data in support of this conclusion.[41]

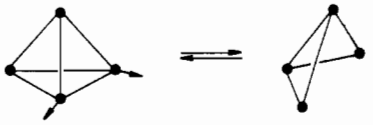

Figure 19. Tetrahedron–butterfly equilibrium for $Pt_4(CO)_5(PPh_3)_4$.

In toroidal gold clusters, there are three S^{σ}, P^{σ}_x, and P^{σ}_y skeletal bonding orbitals, and skeletal rearrangements involving alternative toroidal geometries with the same three bonding orbitals will not involve orbital crossings. Hence, rearrangements in which the geometry remains oblate will be orbital symmetry allowed. However, rearrangements that would interconvert the oblate starting geometry into a prolate spherical cluster, e.g. a pentagonal bipyramid such as $Au_7(PPh_3)_7^+$ into a capped octahedral cluster, are forbidden by orbital symmetry because the latter species would be characterized by occupied S^{σ} and P^{σ}_z orbitals. Since toroidal gold clusters are known to be stereochemically nonrigid, we conclude that the rearrangements must involve transition states with oblate spheroidal geometries. This situation results from the way that the P^{σ} orbitals split in the two topologies and can be rationalized by using a qualitative TSH barycenter rule that is described in the preceding paper.[42] Circumstantial evidence for the soft nature of the potential energy surface in these gold cluster compounds is also provided by the occurrence of skeletal isomers in the solid state.[41]

We might also mention some clusters formed by alkali and alkaline-earth metals, where the p^{π} orbitals of the vertex atoms are again expected to play no part. Such species include CL_6[43] and $BeLi_6$ and $MgNa_6$, which have recently been extensively studied by ab initio calculations.[44] We would clearly expect these clusters to be stereochemically nonrigid too.

Clusters with Capping Group Ib Metal Atoms

Recently a large number of mixed-metal clusters containing $MPPh_3$ (M = Cu, Ag, Au) fragments have been characterized. In these compounds, compact structures based upon face-sharing tetrahedra are generally formed with the $MPPh_3$ fragment capping the least hindered triangular face. When two or more of the $MPPh_3$ fragments are bonded to the cage, they are generally observed to undergo skeletal rearrangements that lead to their site exchange. The remaining part of the cluster skeleton remains rigid throughout this process. As we have previously pointed out,[45] this is a special case of skeletal stereochemical nonrigidity that results from the unusual bonding capabilities of the d^{10} $MPPh_3^+$ fragments. These fragments can form multicentered bonds through an out-pointing s/p_z hybrid with either two or three transition-metal atoms. The fact that $MPPh_3^+$ fragments can function equally well as either face- or edge-bridging groups and in each case increment the total electron count by 12 provides a ready explanation for the stereochemical nonrigidity of such compounds.[46]

Platinum and Palladium Clusters

Palladium and platinum clusters do not have electron-counting rules analogous to those of the boranes and carboranes. The pattern of orbital energy levels characteristic of these species differs significantly from that observed for main-group and transition-

(35) Gladfelter, W. L.; Geoffrey, G. L. *Inorg. Chem.* **1980**, *19*, 2579. Geoffrey, G. L. *Acc. Chem. Res.* **1980**, *13*, 469.
(36) Salter, I. D. *Adv. Dyn. Stereochem.*, in press.
(37) Heaton, B. T.; Strona, L.; Pergola, R. D.; Vidal, J. L.; Schoening, R. C. *J. Chem. Soc., Dalton Trans.* **1983**, 1941.
(38) Garlaschelli, L.; Fumagalli, A.; Martinengo, S.; Heaton, B. T.; Smith, D. O.; Strona, L. *J. Chem. Soc., Dalton Trans.* **1982**, 2265.
(39) Vidal, J. L.; Walker, W. E.; Pruett, R. L.; Schoening, R. C. *Inorg. Chem.* **1979**, *18*, 129.
(40) Mingos, D. M. P.; Johnston, R. L. *Struct. Bonding* **1987**, *68*, 30.
(41) Hall, K. P.; Mingos, D. M. P. *Prog. Inorg. Chem.* **1984**, *32*, 237.
(42) Wales, D. J.; Mingos, D. M. P. *Inorg. Chem.*, preceding paper in this issue.
(43) Schleyer, P. v. R.; Würthwein, E.-U.; Kaufmann, E.; Clark, T. *J. Am. Chem. Soc.* **1983**, *105*, 5930.
(44) Bonačić-Koutecký, V.; Fantucci, P.; Pewestorf, W.; Koutecký, J. *ISSPIC 4 Conference Abstracts*; Universite d'Aix Marseille: Aix-en-Provence, France, 1988; p 60.
(45) Mingos, D. M. P. *Polyhedron* **1984**, *3*, 1289.
(46) Salter, I. D. *Adv. Organomet. Chem.*, in press.

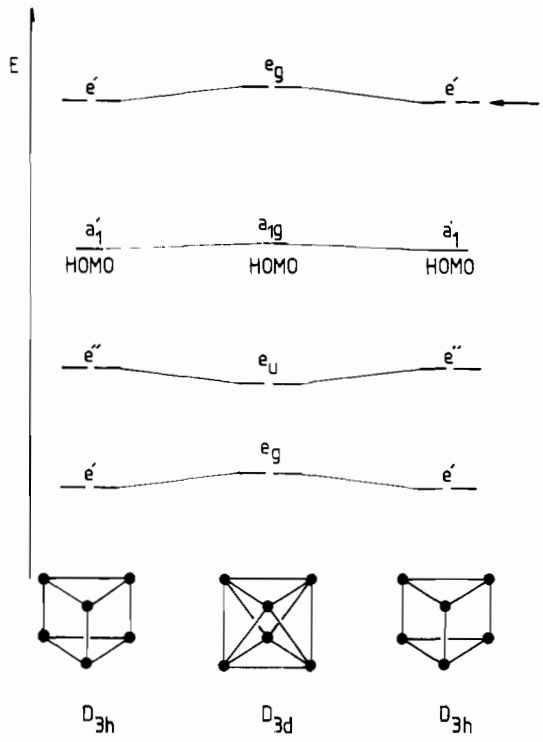

Figure 20. Correlation diagram for the trigonal-twist mechanism for $Pt_6(CO)_{12}^{2-}$. The unoccupied e' orbitals indicated by the arrow correspond to an accessible pair in clusters that follow the PSEPT rules.

metal carbonyl clusters which conform to the PSEPT. As a consequence, some of the rearrangement processes that are unfavorable for $B_nH_n^{2-}$ and, e.g., $[Os(CO)_3]_n$ become energetically feasible. This is illustrated by the observed fluxionality of $Pt_4(CO)_5(PPh_3)_4$ on the NMR time scale.[47] A tetrahedron–butterfly rearrangement has been proposed to account for this observation. For compounds that conform to PSEPT, such a process involves a change in the number of skeletal electron pairs from four to five when one of the metal–metal bonds is broken (Figure 19). Extended Hückel molecular orbital calculations on $Pt_4L_4(CO)_5$ have indicated that the butterfly–tetrahedron rearrangement process has a relatively soft potential energy surface. As the wing-tip atoms are brought closer together, the overlap integrals increase and the out-of-phase linear combination rises in energy. For a main-group tetrahedral cluster, this molecular orbital would become strongly antibonding and make the process symmetry forbidden. For platinum, the smaller d–d overlap integrals and the mitigating effect of the d–p mixing reduce the activation energy.[48]

There is also considerable evidence that in the stacked platinum clusters $[Pt(CO)_3]_n^{2-}$ the platinum triangles rotate relative to one another by a low-energy trigonal-twist mechanism. The process involves an intermediate trigonal prism for octahedra and is not expected to be favorable for either main-group clusters or transition-metal clusters with the normal 86 valence electron count, as discussed above. In the trigonal-prismatic $Pt_6(CO)_{12}^{2-}$, however, the bonding is somewhat different. The valence-shell p orbitals are relatively high in energy for platinum; this leads to rather weak interactions between the two platinum triangles, and there is only one accessible orbital corresponding to bonding between them.[49] Six of the seven skeletal molecular orbitals are strongly bonding within the platinum triangles and only weakly bonding between them; their energies are not sensitive to relative rotation of the triangles. The other, a'_2, bonding orbital also shows little preference for either geometry. Hence, this cluster has only 86 valence electrons, the same as an octahedral cluster such as $Os_6(CO)_{18}^{2-}$, and rearrangements involving involving relative rotation of the $Pt_3(CO)_6$ triangles are therefore facile. The frontier orbitals for this cluster are given in Figure 20. Unlike the situation illustrated in Figure 8, there are no avoided crossings, the two alternative geometries have similar energies, and the twist mechanism has a low activation energy. This result also suggests that ligand disposition can be an important factor in transition-metal rearrangements. Hence $Pt_6(CO)_{12}^{2-}$, where the carbonyls bridge only the triangular edges, is fluxional, but $Os_6(CO)_{18}^{2-}$ is not. In platinum clusters the metal–metal bonding across those edges that are not carbonyl bridged is weak, and consequently the potential energy surfaces for rearrangements involving these edges appear to be soft.

The related trigonal-prismatic clusters $[PtRh_2(CO)_x]_2^-$ appear to undergo a similar fluxional process involving the rotation of $PtRh_2$ triangles. The mixed-metal cluster $PtRh_8(\mu_3\text{-}CO)_3(\mu_2\text{-}CO)_9(CO)_7^{2-}$ has a structure based upon two octahedra sharing a common face. Rotation of the two rhodium triangles about the pseudo-3-fold axis has been proposed as a possible explanation of the observed ^{13}C NMR data.[50]

Conclusions

In this study of cluster fluxionality, we have been concerned mostly with transition-metal clusters, main-group clusters having been discussed at length in part 1.[7] We have discussed some additional single edge-cleavage processes that had not been considered for main-group clusters and have developed the symmetry selection rules of part 1 and a new skeletal electron count selection (SECS) rule. The latter rule is not expected to be as strong as orbital symmetry selection rules as it is based upon the assumed conservation of the number of skeletal electron pairs. It is applied by using the general rules of PSEPT, the capping principle, and the condensation principle to predict the electron counts of suggested transition states or intermediates. An alternative justification of this approach is to reason that if several structures with the same skeletal electron count exist, then fluxionality is more likely to occur.

Having concluded that none of the additional single edge-cleavage processes are likely to be very favorable, we considered more complex mechanisms involving the breaking of more than one edge. Clearly, we would expect these mechanisms to be less favorable than simple DSD processes where these are available. However, we argued that such mechanisms will probably be required to explain any difference in trends of rearrangement rates observed between transition-metal clusters and isostructural main-group clusters, as the TSH symmetry-forced-crossing rule may also be applicable here.

There are also a number of possibilities that do not arise for main-group clusters. These include "radially" bonded clusters, exemplified by various gold clusters, which are all expected to be readily fluxional. Palladium and platinum clusters may also exhibit fluxional behavior because deformations of nonbridged metal–metal bonds have very soft potential energy surfaces. Nido transition-metal clusters may also be able to rearrange by the square–diamond, diamond–square (SDDS) mechanism, where one face opens and another closes.

Last, we should note that there are certain assumptions which were made in applying the SECS rule in a generalized manner to intermediate structure with open faces. For example, in the proposed deltahedron → *nido*-deltahedron + tetrahedral cap process we assumed that the nido cluster would have the usual skeletal electron pair count of $n + 2$, where n is the number of vertices. However, this is clearly not applicable to, for example, the single DSD process in $B_8H_8^{2-}$, where the transition state has an open face. This can be explained because the open face has no bridging protons around it to stabilize an additional orbital. This is not likely to pose such a problem for transition-metal clusters, where such stabilization is not usually required. However,

(47) Moor, A.; Pregasin, P. S.; Venanzi, L. M.; Welch, A. J. *Inorg. Chim. Acta* **1984**, *85*, 103.
(48) Mingos, D. M. P.; Slee, T. Manuscript in preparation.
(49) Underwood, D. J.; Hoffmann, R.; Tatsumi, K.; Nakamura, A.; Yamamoto, Y. *J. Am. Chem. Soc.* **1985**, *107*, 5968.
(50) Fumagalli, A.; Martinengo, S.; Chini, P.; Albinanti, A.; Bruckner, S.; Heaton, B. T. *J. Chem. Soc., Chem. Commun.* **1978**, 195.

clusters with interstitial atoms should be treated with caution, as where we know that open faces may sometimes be present even when there is a closo electron count, e.g. $Rh_{13}(CO)_{24}H_3^{2-}$.

Acknowledgments. We thank Dr. I. D. Salter for kindly providing us with reprints and preprints of his recent papers on stereochemically nonrigid metal clusters. We also thank Dr. A. Rodger and Dr. T. Slee for some helpful discussions. D.J.W. thanks the SERC and Downing College Cambridge for financial support for his stay in Oxford in 1988 during which this work was performed.

Contribution from the Departments of Chemistry, University of Dayton, 300 College Park Avenue, Dayton, Ohio 45469, and Southwest Missouri State University, Springfield, Missouri 65804

Investigation of Lithium-Water Interactions in Acetonitrile Solutions Using Proton Nuclear Magnetic Resonance, Raman, and Infrared Spectroscopies and Extended Hückel Molecular Orbital Calculations

R. Gerald Keil,*,† David W. Johnson,† Mark A. Fryling,† and James F. O'Brien‡

Received February 8, 1989

Exchange of acetonitrile into and out of the coordination sphere of lithium ion is shown to be fast on the NMR time scale and slow on the vibrational time scale. Addition of water to solutions of lithium perchlorate in acetonitrile indicates that lithium is preferentially solvated by water and reveals that the solvation number of lithium ion is 4. Results from NMR, IR, Raman, and extended Hückel molecular orbital calculations are used to discuss the $LiClO_4$-H_2O-CH_3CN system.

Introduction

Lithium has been considered for many years as an anode material for nonaqueous batteries. Acetonitrile (AN) is well suited as a nonaqueous solvent system for electrochemical studies because of its physical properties[1] and because of its ability to dissolve substantial quantities of salts to yield conductive solutions. Its physical properties, including its large electrochemical window, make it most attractive. The reactivity of lithium metal with acetonitrile has compromised AN as a solvent system for batteries. Passivated[2] lithium anodes cause a voltage delay when power is initially drawn, and this lasts until local electrode heating dissipates the film. The recent work by Keisele[3] on the purification of acetonitrile was used as a background for this research. A thorough surface spectroscopic study of the reactivity of lithium metal[4] with gases[5] was recently reported. Information about the physical state of the lithium ion in solution has been obtained from conductance and transference studies[6] of lithium salts in solution. The large charge to volume ratio for lithium makes its chemistry a curiosity. An attempt to obtain knowledge of the interface charge-transfer process must include a study of the lithium ion environment in solution.

Previous studies of lithium ion in aqueous solution have yielded hydration numbers[7] ranging from 2 to 22. Some of the methods employed, notably transference numbers[8] and mobility[9] measurements, clearly measure numbers of solvent molecules beyond the first coordination sphere. NMR results, which usually detect the first solvation shell only, report[10] hydration numbers of 3.4-5.0. In addition, calculated NMR shifts agree with experimental results[11] when a tetrahedral $Li(H_2O)_4^+$ ion is used. A potential energy surface calculation also suggests a four-coordinate T_d geometry for aqueous lithium ion[12] is most stable.

Solvation numbers of lithium ion in acetonitrile range from 4 to 9. Again, conductivity experiments yield the higher[13] values. Spectral measurements based upon infrared peak areas yield a solvation number[14] of 4. Solubility measurements also suggest a solvation number of 4, and $LiClO_4 \cdot 4CH_3CN$ (s) has been isolated.[15]

In a mixed-solvent system containing water and acetonitrile, the lithium ion is preferentially solvated by water. This has been shown by ^7Li NMR[16] and IR[17] measurements. Some workers have suggested that acetonitrile is inert in the presence of water and have made the claim that it is completely displaced by water from the lithium coordination[18] sphere, as it has been shown to displace tetrahydrofuran. Coordination of acetonitrile generally results in a shift of the CN stretching frequency to higher[19] values. Coordination to Zn^{2+}, for example, results in an increase of the CN stretching band[20] of 40 cm^{-1}. Molecular orbital calculations have been used to explain the vibrational[19,21] frequency enhancement. Interaction of CH_3CN with water in the absence of lithium results in an additional IR peak[22] at 2262 cm^{-1}.

* To whom correspondence should be addressed.
† University of Dayton.
‡ Southwest Missouri State University.

(1) Fry, A. J.; Britton, W. F. Solvents and Supporting Electrolytes. In *Laboratory Techniques in Electroanalytical Chemistry*; Kissinger, P. T., Heineman, W. R., Eds.; Marcel Dekker: New York, 1984; p 371.
(2) Pons, S.; Khoo, S. DTIC Technical Report, Government Accession No. AD-A106815; Defense Logistics Agency: Alexandria, VA, 1981.
(3) Keisele, H. *Anal. Chem.* **1980**, *52*, 2230.
(4) Hoenigman, J. R.; Keil, R. G. *Appl. Surf. Sci.* **1984**, *18*, 207.
(5) Hoenigman, J. R.; Keil, R. G. An XPS Study of the Exposure of Lithium to Low Levels of O_2, CO, CO_2, and SO_2. In *Lithium: Current Applications in Science, Medicine and Technology*; Bach, R. O., Ed.; Wiley: New York, 1985; Chapter 17.
(6) Venkatesetty, H. V. *Lithium Battery Technology*; The Electrochemical Society Monograph Series; Electrochemical Society: Pennington, NJ, 1984.
(7) Burgess, J. *Metal Ions in Solution*; Ellis Harwood Ltd.: Chichester, England, 1978; p 141.
(8) Rutgers, A. T.; Hendrikx, V. *Trans. Faraday Soc.* **1962**, *58*, 2184. Remy, H. *Trans. Faraday Soc.* **1927**, *23*, 381.
(9) Robinson, R. A.; Stokes, R. H. *Electrolyte Solutions*, 2nd ed., revised; Butterworth: Boston, MA, 1968; Chapter 5.
(10) Bockris, J. O.; Saluja, P. P. S. *J. Phys. Chem.* **1972**, *76*, 2298.
(11) Akitt, J. W. *J. Chem. Soc., Dalton Trans.* **1973**, 42.
(12) Kollman, P. A.; Kuntz, I. D. *J. Am. Chem. Soc.* **1974**, *96*, 4766.
(13) Hinton, J. F.; Amis, E. S. *Chem. Rev.* **1971**, *71*, 627.
(14) Pevelyin, I. S.; Klinchuk, M. A. *Russ. J. Phys. Chem.* (*Engl. Transl.*) **1973**, *47*, 1138.
(15) Tomkins, R. P. T.; Turner, P. J. *J. Chem. Eng. Data* **1975**, *20*, 50.
(16) Maciel, G. E.; Hancock, J. K.; Lafferty, L. F.; Mueller, P. A.; Musker, W. K. *Inorg. Chem.* **1966**, *5*, 554.
(17) Boran, M. H.; deLoze, C. *J. Chim. Phys. Phys.-Chim. Biol.* **1971**, *68*, 1293.
(18) Stockton, G. W.; Martin, J. S. *J. Am. Chem. Soc.* **1972**, *94*, 6921.
(19) Purcell, K. F.; Drago, R. S. *J. Am. Chem. Soc.* **1966**, *88*, 919.
(20) Purcell, K. F. Ph.D. Thesis, University of Illinois, 1965; p 39.
(21) Evans, J. C.; Lo, G. Y.-S. *Spectrochim. Acta* **1965**, *21*, 1033.
(22) Coetzee, J. F.; Sharpe, W. R. *J. Solution Chem.* **1972**, *1*, 77.

0020-1669/89/1328-2764$01.50/0